

Integrated piezoresistive sensors for atomic force-guided scanning Hall probe microscopy

A. J. Brook, S. J. Bending, J. Pinto, A. Oral, D. Ritchie et al.

Citation: *Appl. Phys. Lett.* **82**, 3538 (2003); doi: 10.1063/1.1576914

View online: <http://dx.doi.org/10.1063/1.1576914>

View Table of Contents: <http://apl.aip.org/resource/1/APPLAB/v82/i20>

Published by the [American Institute of Physics](http://www.aip.org).

Additional information on *Appl. Phys. Lett.*

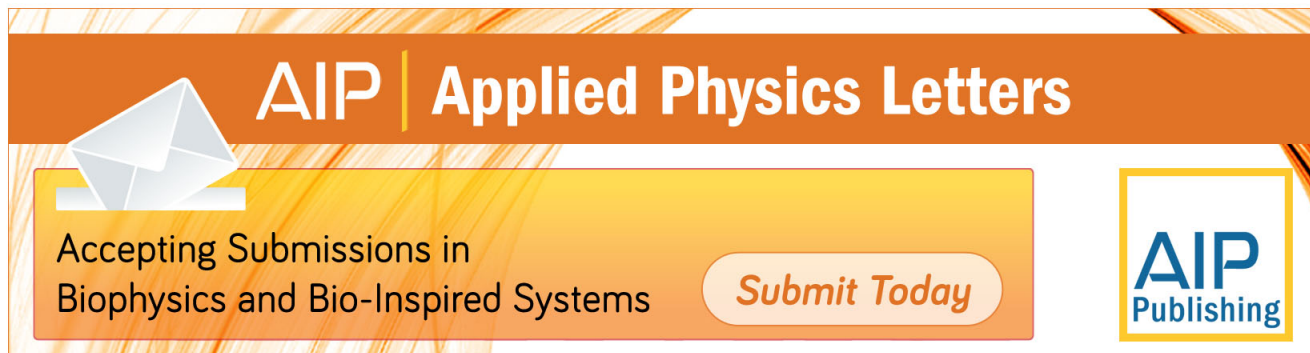
Journal Homepage: <http://apl.aip.org/>

Journal Information: http://apl.aip.org/about/about_the_journal

Top downloads: http://apl.aip.org/features/most_downloaded

Information for Authors: <http://apl.aip.org/authors>

ADVERTISEMENT



AIP | Applied Physics Letters

Accepting Submissions in
Biophysics and Bio-Inspired Systems

Submit Today

AIP
Publishing

Integrated piezoresistive sensors for atomic force-guided scanning Hall probe microscopy

A. J. Brook, S. J. Bending,^{a)} and J. Pinto

Department of Physics, University of Bath, Bath, BA2 7AY United Kingdom

A. Oral

Department of Physics, Bilkent University, 06533 Ankara, Turkey

D. Ritchie and H. Beere

Cavendish Laboratory, Cambridge University, Cambridge, CB3 0HE United Kingdom

M. Henini

Department of Physics, University of Nottingham, Nottingham, NG7 2RD United Kingdom

A. Springthorpe

Nortel Networks Optical Components Inc., 3500 Carling Avenue, Ottawa, Ontario K2H 8E9, Canada

(Received 21 October 2002; accepted 31 March 2003)

We report the development of an advanced sensor for atomic force-guided scanning Hall probe microscopy whereby both a high mobility heterostructure Hall effect magnetic sensor and an $n\text{-Al}_{0.4}\text{Ga}_{0.6}\text{As}$ piezoresistive displacement sensor have been integrated in a single III–V semiconductor cantilever. This allows simple operation in high-vacuum/variable-temperature environments and enables very high magnetic and topographic resolution to be achieved simultaneously. Scans of magnetic induction and topography of a number of samples are presented to illustrate the sensor performance at 300 and 77 K. © 2003 American Institute of Physics.

[DOI: 10.1063/1.1576914]

The demonstration of $p\text{-Si}$ atomic force microscopy (AFM) cantilevers with piezoresistive detection¹ represented a major milestone in the field of scanning probe microscopy as it allowed variable temperature atomic-resolution topographic imaging without the need for optical sensing elements with precise alignment criteria. There is much to be gained by the extension of piezoresistive detection to III–V semiconductor cantilevers since it would allow one to exploit the direct band gaps and high carrier mobilities in these materials. In particular scanning tunneling microscope (STM)-guided scanning Hall probe microscopy (SHPM),^{2,3} which is noninvasive and yields quantitative low-noise magnetic images, could be extended to nonconducting or electrically unconnected samples. While the use of GaAs as a piezoresistive material has been limited by its low piezoresistive coefficient,⁴ the Al content of $n\text{-Al}_x\text{Ga}_{1-x}\text{As}$ alloys can be tailored to give large piezoresistive coefficients.⁵ We have recently shown that high sensitivity piezoresistive detection can be achieved using a cantilever with an $n\text{-Al}_{0.4}\text{Ga}_{0.6}\text{As}$ layer as the piezoresistive sensing element.⁶ Since our sensor is composed exclusively of $\text{Al}_x\text{Ga}_{1-x}\text{As}$ alloy layers, which can be grown with almost perfect epitaxy, it allows us to realize an integrated low-noise Hall probe in a high-mobility $\text{Al}_{0.3}\text{Ga}_{0.7}\text{As}/\text{GaAs}$ two-dimensional electron gas (2DEG) grown at the surface of the cantilever.

Figure 1(a) shows a scanning electron micrograph of a completed cantilever revealing the two primary sensors required for dual magnetic and topographic imaging. The first sensor, a Hall cross [inset Fig. 1(a)] situated near the very

end of the cantilever, is electrically contacted via the four gold leads at either side of the cantilever. The piezoresistor is placed at the base of the cantilever where bending stresses are at a maximum. In addition a sharp ($< 100\text{ nm}$ diameter) AFM tip has been micromachined at the very end of the

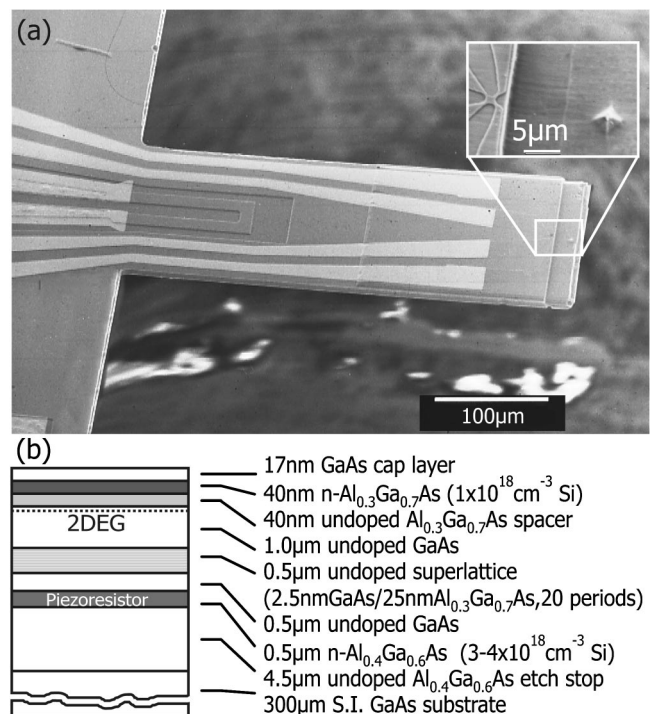


FIG. 1. (a) SEM of a fabricated piezoresistive cantilever. Inset shows a blow up of the Hall probe and pyramidal AFM tip. (b) Epilayer structure for our integrated cantilever.

^{a)}Electronic mail: pyssb@bath.ac.uk

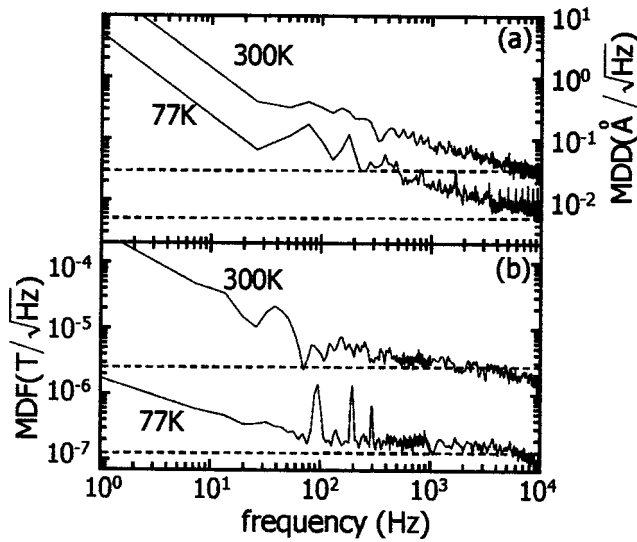


FIG. 2. Measured noise spectra of (a) the piezoresistor and (b) the Hall sensor at 300 K and 77 K. Dotted horizontal lines indicate the Johnson noise limits.

sensor, close to the Hall probe. The entire cantilever has been fabricated from a single GaAs/AlGaAs epilayer structure [sketched in Fig. 1(b)], grown by molecular beam epitaxy at 590 °C. From top to bottom the stack comprises a modulation doped $n\text{-Al}_{0.3}\text{Ga}_{0.7}\text{As}/\text{GaAs}$ structure forming a 2DEG ~ 100 nm from the surface which is separated from the $n\text{-Al}_{0.4}\text{Ga}_{0.6}\text{As}$ piezoresistive layer by an electrical isolation region composed of two undoped GaAs layers and an $\text{Al}_{0.3}\text{Ga}_{0.7}\text{As}/\text{GaAs}$ superlattice. The micromachining steps developed to realize the cantilever are reported elsewhere.⁶

The performance of the cantilever as an AFM sensor can be estimated from its geometry and material properties. For the rectangular cantilever shown in Fig. 1(a) the spring constant is well described by

$$k = \frac{Ewt^3}{4L^3}, \quad (1)$$

where t is the thickness, w is the width, L is the length of the cantilever, and E is the Young's modulus in the [011] direction ($E = 12.2 \times 10^{10}$ Pa).⁷ The fractional resistance change is given by

$$\frac{\Delta R}{R} = \frac{3\pi_L Et[1 - l/(2L)](1 - t_r/t)}{2L^2} \Delta z, \quad (2)$$

where Δz is the deflection of the cantilever tip, t_r is the thickness of the piezoresistor, and π_L is the longitudinal piezoresistive coefficient. Using our known cantilever dimensions ($L = 400 \mu\text{m}$, $w = 150 \mu\text{m}$, $t = 6 \mu\text{m}$, $l = 60 \mu\text{m}$, and $t_r = 0.5 \mu\text{m}$) and piezoresistive coefficient ($\pi_L = 1.35 \times 10^{-9} \text{ Pa}^{-1}$ in $n\text{-Al}_{0.4}\text{Ga}_{0.6}\text{As}$ at 300 K)^{6,8} we calculate that $k \cong 15 \text{ N/m}$ and $\Delta R/(R\Delta z) = 8.0 \times 10^{-7} \text{ \AA}^{-1}$. The figure-of-merit of AFM sensor performance is the minimum detectable deflection (MDD) whose fundamental limit is set by the Johnson noise ($V_n = \sqrt{4k_B TR \Delta f}$) from the piezoresistor and the three identical resistors in the Wheatstone bridge into which it is incorporated. We estimate a MDD of $0.02 \text{ \AA}/\sqrt{\text{Hz}}$ at 300 K for a typical piezoresistor with resistance 25 k Ω .

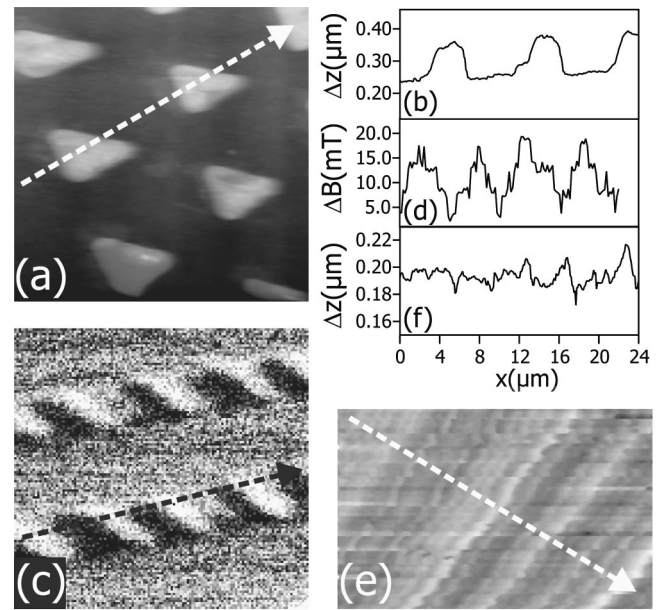


FIG. 3. (a) AFM image of an hexagonal array of Au triangles [image size (IS) $\sim 20 \mu\text{m} \times 20 \mu\text{m}$, grayscale spans (GS) ~ 100 nm]. (b) Linescan in the direction indicated in (a). (c) Magnetic image of a magnetic imaging reference sample (MIRS) (IS $\sim 20 \mu\text{m} \times 18 \mu\text{m}$, GS ~ 18 mT). (d) Linescan of (c) in direction indicated. (e) Topographic image of MIRS (IS $\sim 20 \mu\text{m} \times 12 \mu\text{m}$, GS ~ 100 nm). (f) Linescan in direction indicated in (e).

The performance of the Hall probe is also determined by its dimensions and the Johnson noise limit. The x - y resolution of the sensor shown in Fig. 1(a) is limited to $\sim 1 \mu\text{m}$ by the optical lithographic processing, although submicron probes could easily be realized by electron-beam lithography. The Johnson noise-limited minimum detectable field is given by $B_{\min} = \sqrt{4k_B TR \Delta f} / I_H R_H$ where R is the series resistance of the voltage leads, I_H is the Hall current and the R_H Hall coefficient. For a $1 \mu\text{m}$ Hall cross, with typical values of $R = 80 \text{ k}\Omega$, $R_H = 3000 \Omega/\text{T}$, and $I_H = 4 \mu\text{A}$ at 300 K, a MDF of $3 \times 10^{-6} \text{ T}/\sqrt{\text{Hz}}$ is estimated.

Plots of measured noise spectra for the piezoresistor and Hall probe at 300 and 77 K are given in Figs. 2(a) and 2(b). At low frequencies $1/f$ noise dominates the response of both piezoresistor and the Hall probe, while above a corner frequency the indicated Johnson noise limit is rapidly approached. The noise figures fall abruptly when the sensor is cooled to 77 K due to the explicit temperature dependence of the Johnson noise as well as that of the piezoresistive coefficient and the resistance of the Hall probe leads.

Measurements were performed with the cantilever mounted in a low temperature STM which had been modified for AFM use. The deflection of the cantilever was measured in a Wheatstone bridge driven at 5 V dc, composed of the piezoresistor and three almost identical resistors. The output was passed through a low noise high gain amplifier and detected with a phase sensitive detector. The resonant frequency of our cantilevers ranged from 18 to 21 kHz and quality factors of 300–500 could be achieved in air ($Q > 10\,000$ under vacuum).

The cantilever was tested in AFM mode by scanning a patterned 100-nm-thick gold film comprising of triangles (side length $5 \mu\text{m}$) in a hexagonal array with $10 \mu\text{m}$ period

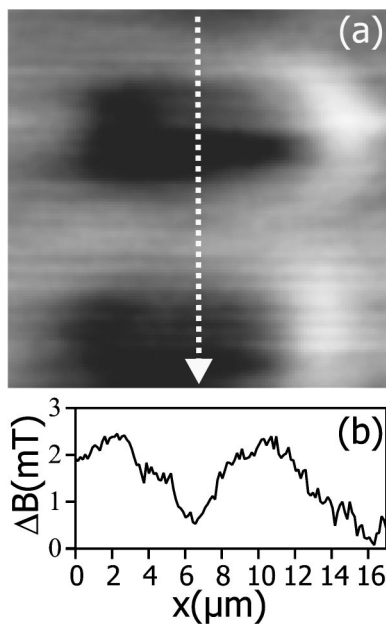


FIG. 4. (a) Magnetic image of a square array of YBCO squares (IS $\sim 16 \mu\text{m} \times 16 \mu\text{m}$, $G_S \sim 2.5 \text{ mT}$), $T = 77 \text{ K}$, $\mu_0 H_z = 2.5 \text{ mT}$. (b) Linescan in the direction indicated in (a).

along a given lattice vector [Fig. 3(a) and linescan in Fig. 3(b)]. The image was scanned in noncontact mode with the cantilever slightly inclined ($1^\circ - 2^\circ$) with respect to the sample. The cantilever was oscillated close to its resonance frequency and approached towards the sample until the oscillation amplitude dropped to a predetermined value. The z motion of the scanner tube was then used to keep this amplitude constant while scanning the sample surface.

Figure 3(c) shows a scan of the local induction at the surface of a magnetic imaging reference sample⁹ at 300 K. The sample is a high density data storage disk with a complex bit track written on it with a repeat distance of $\sim 10.5 \mu\text{m}$. Two bit tracks are clearly resolved with the expected repeat distance as illustrated in the linescan shown in Fig. 3(e). Figure 3(d) is a topographic image of a small region of the same sample showing striping due to laser texturing performed prior to writing the bit track in order to smooth the film [see also linescan in Fig. 3(e)].

Figure 4(a) shows a 77 K magnetic image of part of a 10 μm period square array of 5 μm superconducting $\text{YBa}_2\text{Cu}_3\text{O}_{7-\delta}$ (YBCO) squares. The 0.35- μm -thick (001) YBCO film was grown on a MgO substrate at 690 $^\circ\text{C}$ by electron beam coevaporation of the metals. It was patterned using optical lithography and Ar ion milling, and subsequently annealed in atomic oxygen to optimize the stoichiometry. The sample was zero field cooled to 77 K when a 2.5 mT field was applied perpendicular to the film. The sensor was then scanned across the sample at a constant height of $\sim 1 \mu\text{m}$. Dark areas where the YBCO squares have screened the penetration of flux are clearly resolved, and are seen more clearly in the adjacent linescan [Fig. 4(b)].

In conclusion we have demonstrated an advanced integrated sensor based around a III-V cantilever with piezoresistive detection, which allows one to perform AFM-guided scanning Hall Probe microscopy. In this way the unique advantages of SHPM can be extended to the imaging of nonconducting or unconnected magnetic samples. The sensor's ability to produce simultaneous topographic and magnetic images has been demonstrated. Finally, we note that our piezoresistive cantilever also allows the direct integration of other secondary III-V sensors during epitaxial growth which can further exploit the properties of direct gap semiconductors, e.g., a vertical cavity surface emitting laser or a single electron transistor.

The authors acknowledge the financial support of EPSRC in the UK (Grant No. GR/M76119) and TÜBİTAK in Turkey (Grant No. TBAG-1878).

¹M. Tortonese, H. Yamada, R. C. Barrett, and C. F. Quate, *Proceedings of Transducers '91* (IEEE, New York, 1991), Vol. 91 CH2817-5, p. 448.

²A. M. Chang, H. D. Hallen, L. Harriot, H. F. Hess, H. L. Loa, J. Kao, R. E. Miller, and T. Y. Chang, *Appl. Phys. Lett.* **61**, 1974 (1992).

³A. Oral, S. J. Bending, and M. Henini, *Appl. Phys. Lett.* **69**, 1324 (1996).

⁴A. Dehe, K. Fricke, K. Mutamba, and H. Hartnagel, *J. Micromech. Microeng.* **5**, 139 (1995).

⁵K. Hjort, J. Soderkvist, and J. Schweitz, *J. Micromech. Microeng.* **4**, 1 (1994).

⁶A. J. Brook, S. J. Bending, J. Pinto, A. Oral, D. Ritchie, H. Beere, A. Springthorpe, and M. Henini, *J. Micromech. Microeng.* **13**, 1 (2003).

⁷Calculated from parameters given in, S. Adachi, *J. Appl. Phys.* **58**, R1 (1985).

⁸Measured value from 2.5- μm -thick $n\text{-Al}_{0.4}\text{Ga}_{0.6}\text{As}$ ($1 \times 10^{19} \text{ cm}^{-3}$ Si doped) epilayer at 300 K.

⁹P. Rice, S. E. Russek, J. Hoinville, and M. H. Kelley, *IEEE Trans. Magn.* **33**, 4065 (1997).